The Journal of Engine Research

Journal Homepage: www.engineresearch.ir

Technical Report

Failure analysis of a dynamometer drive shaft coupled to an engine

M. Azadi[1*], R. Rohani[2], M. Roozban[3], A. Mafi[4]

[1]*Irankhodro Powertrain Company (IPCO), Tehran, Iran, m_azadi@ip-co.com*
[2]*Irankhodro Powertrain Company (IPCO), Tehran, Iran, r_rohani@ip-co.com*
[3]*Irankhodro Powertrain Company (IPCO), Tehran, Iran, m_roozban@ip-co.com*
[4]*Irankhodro Powertrain Company (IPCO), Tehran, Iran, a_mafi@ip-co.com*
[*]*Corresponding Author, Phone Number: +98-910-210-7280*

ARTICLE INFO

Article history:
Received: 08 March 2014
Accepted: 19 April 2014

Keywords:
Failure analysis
Dynamometer drive shaft
Fatigue lifetime
Misalignment
Resonance

ABSTRACT

A typical dynamometer drive shaft was damaged during its working condition. This failure was repeated in four cases. In the present article, a failure analysis of a dynamometer drive shaft has been performed. To analyze the failure, the material investigation was carried out by scanning electron microscopy (SEM) images. Additionally, the micro-structure of the failed coupling shaft was photographed, the hardness was measured and compared to properties of the original material. Besides, the fatigue lifetime was calculated based on the high cycle fatigue (HCF) regime and the fatigue endurance limit by simulating the misalignment in a finite element (FE) model. The possibility of torsional vibrations and the occurrence of the resonance condition were also studied. Finally, vibration-monitoring practices were done to compare the vibration amplitudes to an acceptable criterion. SEM images showed cleavage marks under fatigue loadings. These marks indicated the brittle behavior of the material. The micro-structure together with the hardness of the alloy was satisfied. Based on numerical results, the fatigue lifetime of the coupling was likely to terminate according to the misalignment increase, as a cause of the failure. The other cause could be the resonance and the shaft critical speed, which was calculated below the idle speed of engines.

1) Introduction

Dynamometers have been used for starting engines and also endurance or functional testing in test beds. Usually, a drive shaft connects the engine into the dynamometer. Based on this coupling, it is supposed to work under cyclic torsional loadings. Therefore, the fatigue lifetime and vibration phenomenon are important in this component. For this purpose, this component is usually made of a titanium alloy (the Ti-6Al-4V alloy), which has a proper ratio of the strength to the weight.

Such instruments are exposed to torsional cyclic loadings in the high cycle fatigue (HCF) regime. In a typical vehicle installation, the driveline contains an engine coupled to a clutch, a gearbox, a differential system, drive shafts and finally wheels. In an engine test bed, the engine will be directly connected to the dynamometer by means of a coupling system. This coupling system mainly consists of a driveshaft and one or two flexible elements at ends.

This kind of testing machine is quite rugged and insensitive, however some important considerations should be observed to prevent following problems.

- Catastrophic driveline failure
- Engine damage-bearing failure
- Dynamometer damage-bearing failure, drive hub damage and electrical failure
- Excessive engine vibration

In the current case, internal combustion engines are connected to dynamometers by means of a highly flexible coupling system. Failures in similar couplings were repeated four times according to the following chronological order.

- The coupling number 1 was failed after 4526 hrs working (about 4 years).
- The coupling number 2 was failed after 1763 hrs working (about 4-5 years).
- The coupling number 3 was failed after 742 hrs working (about 9 months).
- The coupling number 4 was failed after 2700 hrs working (about 1.5 years).

Root causes were analyzed in a fishbone diagram, shown in Figure 1. As illustrated, the coupling failure can happen in three parts including the shaft bar, elastomer parts and CV-joint components. For each component, there exist several reasons for the failure. For elastomer parts (rubber elements), the environment can be a cause for the failure such as the overheating effect and existing aggressive fluids. The Hertzian stress, the grease quality, the residual imbalance, the misalignment and material defects can be reasons for the failure in CV-joint components. For the shaft failure, one reason can be poor fatigue properties under torsional and bending loads. Other important reason can be the misalignment and the imbalance, when the coupling system is assembled between the dynamometer and the engine.

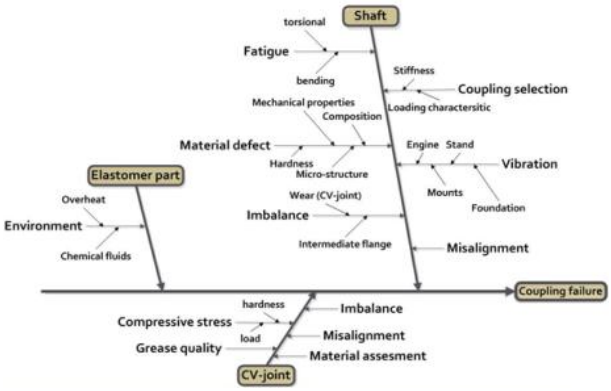

Figure 1: The fishbone for the failure of the coupling system

Furthermore, the incorrect selection of the coupling system can be another main reason of the failure, not only because of loading characteristics, but also because of torsional vibrations. Material defects including unsatisfying the hardness, poor mechanical properties, incorrect element compositions and micro-structures can result in the failure.

In the present research, only causes of the shaft catastrophic failure have been studied, since there were no failures in elastomer parts and the CV-joint component. Based on the fishbone diagram, various works were conducted, as the solving methodology to find the root cause of the failure. They could be listed as follows,

- Material investigations
  - Measuring the chemical composition of the component and comparing to its specification
  - Measuring the hardness of the component and comparing to its specification
  - Checking the micro-structure of the component to verify its production process
  - Checking scanning electron microscopy (SEM) images of the fracture surface to find failure causes
- Mechanical investigations
  - Calculating the vibration behavior (including the natural frequency) of the component to find the critical speed
  - Measuring the vibration spectrum (including the transient behavior) of the component, connected to the engine at various engine speeds
  - Calculating the stress and predicting the fatigue lifetime of the component under various critical loading conditions to find effects of the misalignment and the torque enhancement

2) Observation Results

The highly flexible coupling system, which had been verified appropriately for determined test procedures and certain internal combustion engines, has failed on several occasions. A schematic picture of the engine test bed, the coupling system and its components are shown in Figure 2. The coupling system contains three major components: the titanium alloy bar shaft, engine-side joints (including the CV-Joint components and the boot) and dynamometer-side joints (which was composed of elastomer parts, the friction bearing system, the trunnion, the casing system and the hub). Figure 3 illustrates an example of these coupling systems, in which the shaft was failed after 1200 hrs operation. As it can be seen, a longitudinal crack was distantly stretched through the shaft.

The root cause analysis of the fracture in the coupling system highlighted the role of vibrations as a main problem in malfunctioning of the shaft. Since the torsional vibration is known as a key factor in the fracture of shafts, this is more preferable to cover this area of thought, rather than studying the vibration in general. However, unbalanced components, the misalignment of the driveline, the design of mountings, induced oscillations of the engine and etc. are definitely some main factors of vibrations.

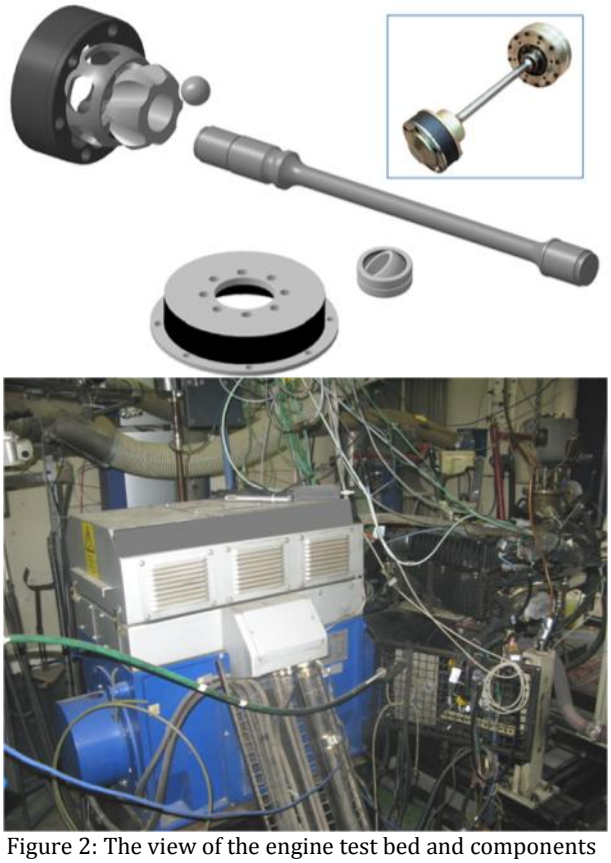

Figure 2: The view of the engine test bed and components of the coupling system

Figure 3: A failed coupling system after 1200 hrs operation

This is the nature of any engine test stand that the isolation of vibrations in any kind is definitely impossible. This is also necessary to notice that the unsatisfactory torsional behavior is not only associated with the coupling system, but also with the whole system including the engine and the dynamometer. However, each component may be quite satisfactory in itself [1].

In spite of the importance of other related parameters, two factors seem to be at the center of attentions. These factors are experimentally proved among careful theorists regarding to considerations in the design of drivelines; critical speeds and the moment of inertia of the engine in comparison to that value of the dynamometer. The easiest way to calculate critical speeds of a coupling system is to use the so-called two-mass system, in which the engine is at one side, the dynamometer exists at the other side and all other elements of the drive chain will be placed between these two masses.

3) Results and Discussions

3.1) Material Investigations

The shaft of the coupling system was made of the Ti-6Al-4V alloy. This titanium alloy has been widely used in industries due to their high strength to weight ratio, good corrosion resistance, excellent fracture toughness and attractive mechanical properties [2].

The chemical composition of the material of the failed drive shaft was determined by a spectrographic chemical analysis method. These results are depicted in Table 1. As illustrated, the coupling alloy was conformed to the standard of the Ti-6Al-4V alloy [3]. Therefore, there was no problem with the coupling material.

Hardness Rockwell C (HRC) tests have been performed by means of a diamond indenter, with 150 kg for 10 s interval on the specimen surface [4]. The hardness was measured as 34, 35, 36, 35 and 34 HRC. It should be mentioned that the average

hardness of the material could be determined to be 34.8 HRC, which was in the range of the specification; 34 to 38 HRC [5]. Thus, there was no doubt about the material hardness, which was a branch of the fishbone diagram, as shown in Figure 1.

In order to investigate the micro-structure and the heat treatment of the coupling material, a part of the shaft near the cracked zone was separated. Micro-structural pictures were taken by a light microscope after grinding, polishing and etching the specimen surface in the Keller's reagent for 30 s [6].

In Figure 4, it can be seen that the micro-structure of the coupling material consisted of α and β phases, in which the distribution of the β phase was proper in the α solid phase [2]. Therefore, the micro-structure of the material (mentioned as a branch in the fishbone diagram) could not be a reason of the failure.

Table 1: Chemical compositions of the failed shaft

Elements	Coupling	Standard [3]
Al	6.3	5.5-6.7
V	4.1	3.5-4.5
Cr	0.020	-
Fe	0.1	Max. 0.4
Nb	0.025	-
Mn	0.015	-
Cu	0.020	-
Ti	Base	Base

Figure 4: The microscopic image of the coupling material near a cracked zone

Effectively, the micro-structure resembled to the heat-treated Ti-Al6-V4 alloy. Micro-structural images of the Ti-6Al-4V alloy, with and without heat treatment are demonstrated in Figure 5, which shows the effect of the heat treatment process on the material micro-structure of the component. It should be born in the mind that the heat treatment of the alloy includes a solution at 950°C for 1 hr, water quenching and ageing at 550°C for 2 hrs [5].

To investigate the cracked zone more accurately, the fracture surfaces were studied under a SEM. Their results are shown in Figure 6 with various magnifications to highlight micro-cracks. It could be predicted that cracks were initiated due to torsional or bending fatigue loadings. Figure 7 demonstrates the fracture surface, containing cleavage marks [7], which shows the brittle fracture.

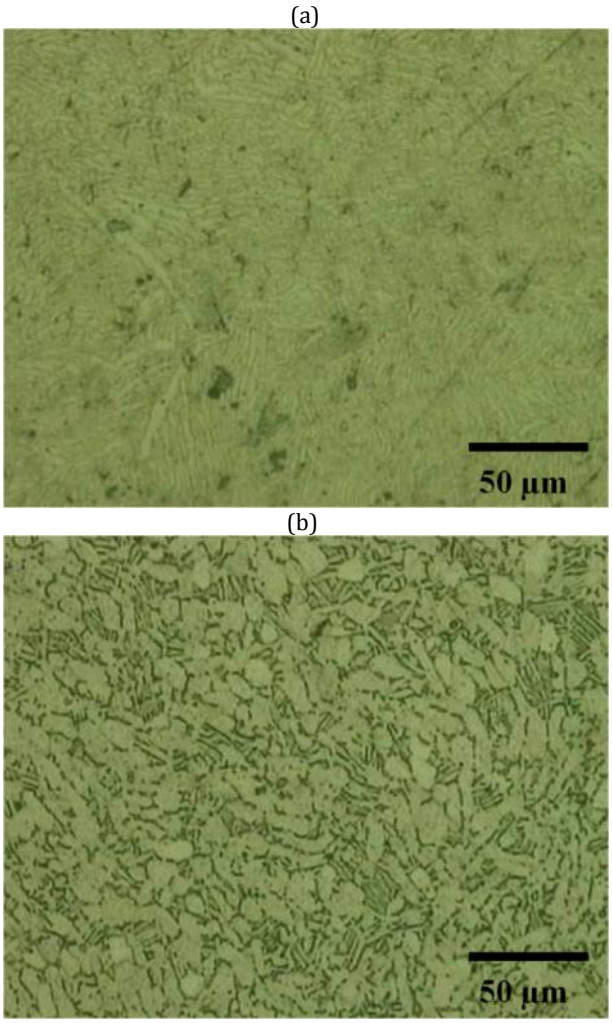

Figure 5: Microscopic images of the Ti-Al4-V6 alloy; including (a) as-received and (b) heat-treated ones

(a)

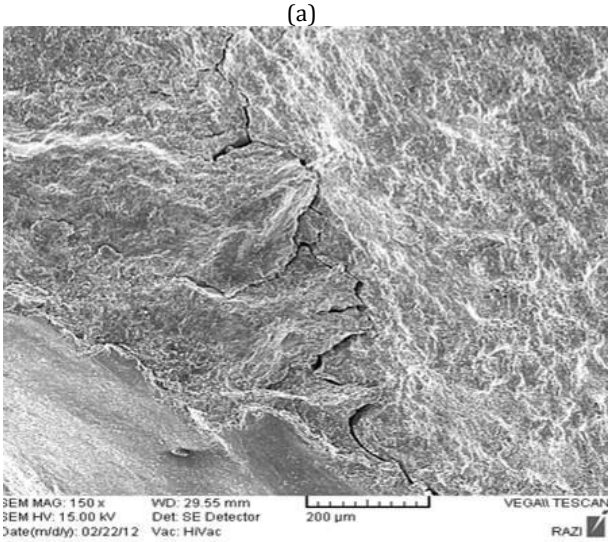

(b)

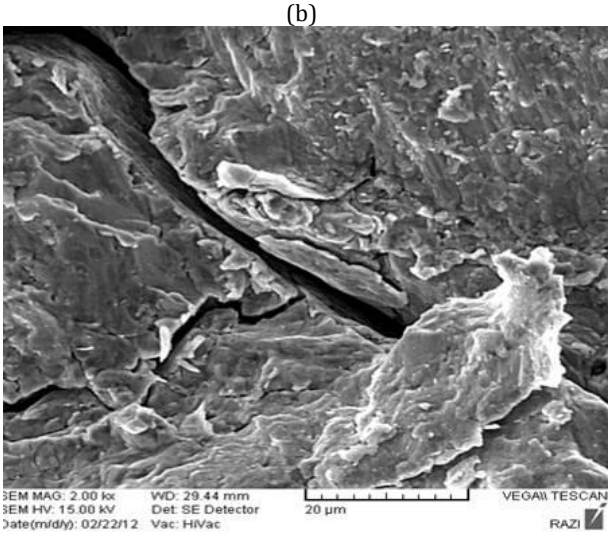

Figure 6: SEM images from cracked zones of the shaft with various magnifications

(a)

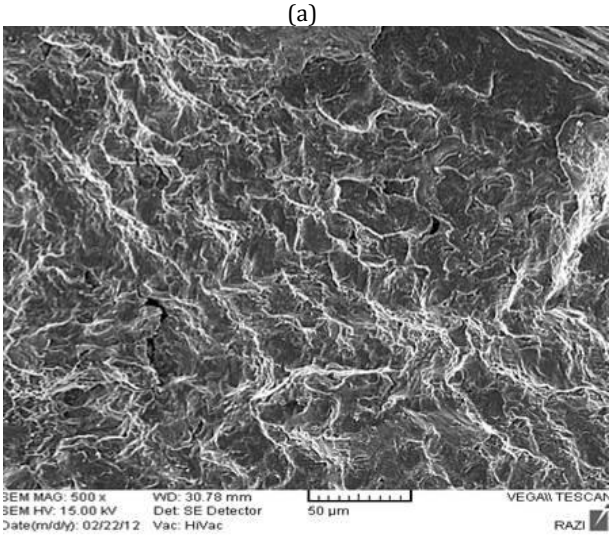

(b)

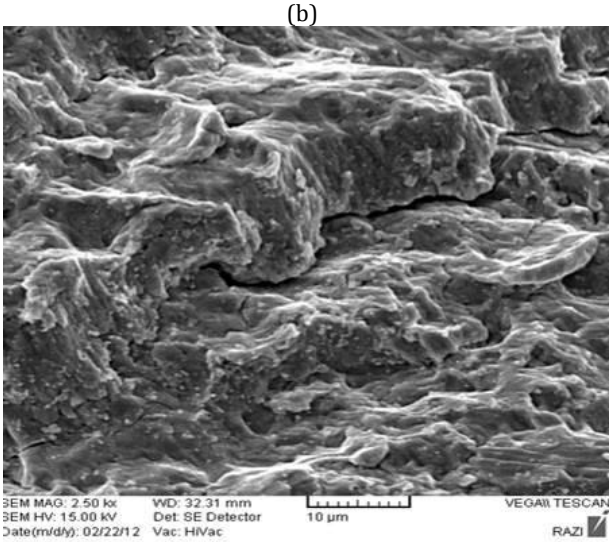

Figure 7: SEM images from fracture surfaces including cleavage marks with various magnifications

Therefore, in the part of material investigations, we could say that:

- Measuring the chemical composition of the component showed that there was an agreement between obtained results and the specification.
- Measuring the hardness of the component demonstrated that the measured value was in the mentioned range of the specification.
- Checking the micro-structure of the component illustrated that the production process could be verified and the heat treatment process seemed to be correct.
- Checking SEM images of the fracture surface showed cleavage marks and the brittle type of the fracture.

Consequently, the branch of the material defect in the fishbone diagram could not be the cause of the failure.

3.2) Mechanical Investigations

To study the vibration behavior, the critical speed should be calculated. The so-called two-mass system formulation to calculate the resonant frequency of the torsional vibration of the system is shown in Equation (1), as reported in the literature [1].

$$n_c = \frac{60}{2\pi}\sqrt{\frac{C_c\left(I_e + I_d\right)}{I_e I_d}} \qquad (1)$$

In which, I_e and I_d are the effective moment of inertia of the engine-side and the dynamometer-side, respectively. And C_c is the torsional stiffness of the shaft. Table 2 represents the moment of inertia of the engine and the dynamometer. Considering I_e = 0.218 kgm^2, I_d = 0.371 kgm^2 and C_c = 1150 Nm/rad, the critical speed could be calculated as 875 cpm. This value was related to a four-cylinder, four-stroke engine with a maximum speed of approximately 6500 rpm.

Table 2: The moment of inertia of the engine and the dynamometer

Engine-side		Dynamometer-side	
Components	Moment of inertia (kgm^2)	Components	Moment of inertia (kgm^2)
Engine	0.137	Dynamometer	0.352
Flywheel adaptor	0.073	Dynamometer adaptor	0.005
Coupling half-1	0.008	Coupling half-2	0.014
Total	0.218	Total	0.371

In general, this is proved that the first resonant speed will occur at the second order for similar cases. It means that when this engine reaches to the speed of 438 rpm, it becomes prone to resonate. According to a general rule, it is good practice to pass the engine speed between 0.8 and 1.2 times of the critical speed as quickly as possible [1, 8]. It means that the speed range of 350-526 rpm for this case needs a certain care.

The direct connection of the engine and the dynamometer leads to the shaft resonance, when the critical speed is situated at the operation range or near it. One way to put this frequency below the idle speed is to use elastomer parts. An elastomer damper in the shape of a rubber ring with a hardness of 50 shore-A at the dynamometer-side of the highly flexible coupling system is a common practice, which will basically shift the critical frequencies of the drive line to out of the normal operation range of the engine. An essential point is that even though the utilization of elastomer parts reduces the possibility of the resonance, the ambient temperature can change the critical speed range. Exceeding a permissible temperature (about 85°C for the natural rubber) shall be prevented [8]. In this case, no sign of overheating was observed and the hardness and the torsional stiffness have not experienced any change.

Besides, the start process shall be done in a quick way preferably less than 1 s [8] to certainly hinder unexpected exceeding of cranking the speed that would expose the coupling system to the catastrophic failure. Unfortunately, there is ample evidence that shows different reasons have lengthened this stage of tests. This fact increases the possibility of the failure due to consequences of this slow transition. As a result, this could be one reason of the failure in the coupling system.

According to the operating manual of dynamometers, the vibration amplitude on bearing spots should be in the following range [8].

- The vibration velocity (alone) should be less than 2.5 mm/s.
- The total vibration velocity should be less than 7 mm/s.

To make sure about the health of machines in this aspect, the vibration velocity was monitored in *Z*-axis in different engine conditions (shown in Figure 8).

In Figure 9, three vibration spectrums in 4000, 5000 and 6000 rpm of the engine speed are shown. In all of them, no extra vibration could be reported. This test has been performed for different situations. The vibration velocity was lower than the value, mentioned before as a criterion. Moreover, vibration picks in Figure 9 are mainly due to the residual imbalance, the small misalignment and combustion knocks, which could be negligible.

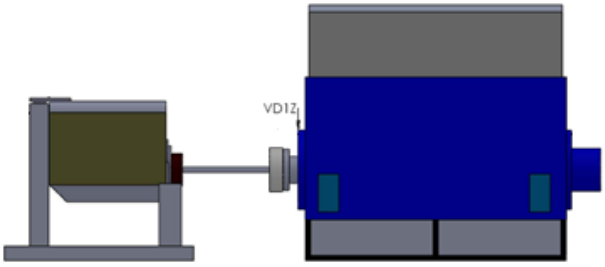

Figure 8: Vibration monitoring on the dynamometer

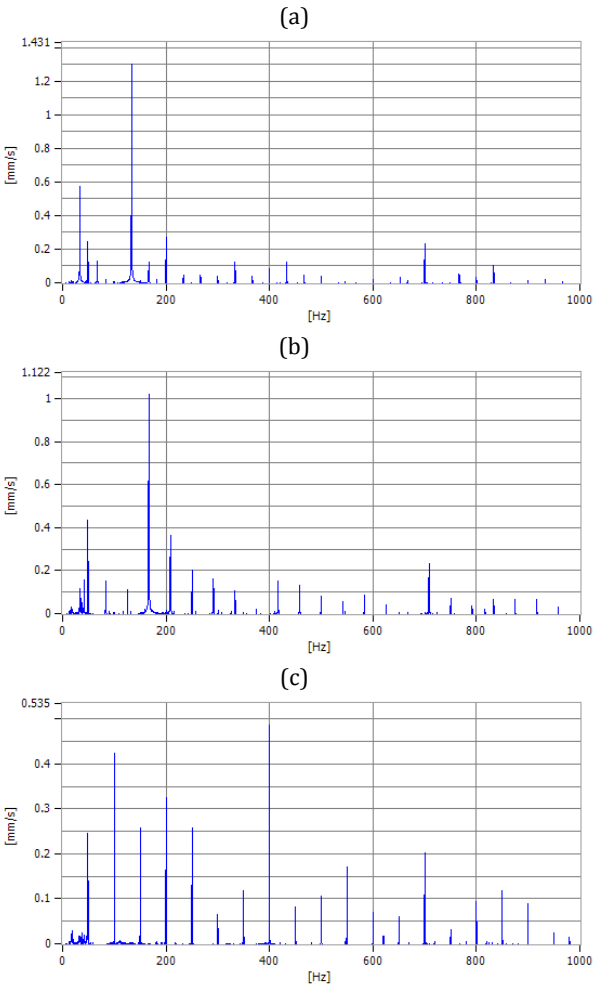

Figure 9: The vibration spectrum measured at (a) 4000 rpm, (b) 5000 rpm and (c) 6000 rpm of the engine speed

For further investigations, the finite element (FE) analysis of the coupling system has been performed by the ABAQUS software. A three-dimensional model of the shaft was meshed by using the C3D8R element (shown in Figure 10). In Figure 10, surfaces of boundary conditions and loadings (the torque and the displacement) are demonstrated. The meshed model includes 82211 elements, 91528 nodes and 280314 degrees of the freedom.

The material was made of the Ti-6Al-4V alloy. Its elastic modulus and Poison's ratio were 110 MPa and 0.31, respectively [5]. An external torque of 400 Nm and a displacement of 0.2 mm (as the misalignment) in *X* direction are applied to the one side of the model and the surface in the other side of the model was fixed in *X* and *Y* directions. It should be mentioned that the applied torque introduces loadings from the engine and the applied displacement namely represent the driveline misalignment.

Figure 11 demonstrates FE results including Von-mises and Tresca stresses. These results are related to 400 Nm torque. The maximum Tresca stress was calculated as 635.7 MPa in comparison to 550.5 MPa of the Von-mises stress. It means that the Tresca stress is more than the Von-mises stress, since the torsional stress is considered by the difference of maximum and minimum principal stresses in the Tresca criterion.

As an important note, to account torsional loading in the coupling system, the Tresca approach is preferable to the Von-mises approach for the mechanical analysis. Based on Von-mises criterion, considering 786 MPa yield strength of the shaft alloy [5], the safety factor could be calculated as 1.43. Having used the Tresca criterion, the safety factor becomes 1.24. Thus, the coupling shaft could withstand more than 400 Nm torque, statically.

Appling 0.2 mm displacement, as an allowable misalignment reported in the literature [8], in addition to 400 Nm torque to the FE model, shows no significant changes on stresses. These results are shown in Table 3. However, by increasing the torque to 500 Nm and the misalignment to 20 mm, stresses change. Raising the torque by 25% will intensify stresses by 25%, according to the linear behavior of the material. A 100 times bigger displacement will increase the Von-mises stress by 20% and the Tresca stress by 15%. If there is an over-range permanent displacement during the operation, the service lifetime of the shaft will reduce by 95% [7]. A radial misalignment less than 0.2 mm is allowed between the engine axis and the dynamometer flange center [7].

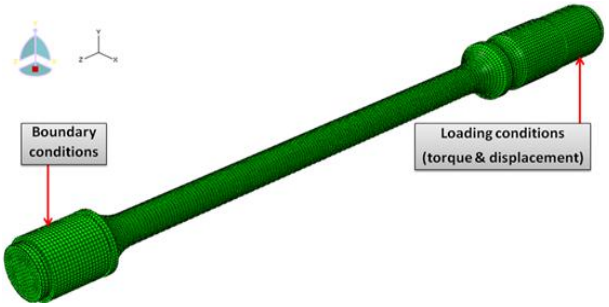

Figure 10: The meshed model of the shaft in the ABAQUS software

(a)

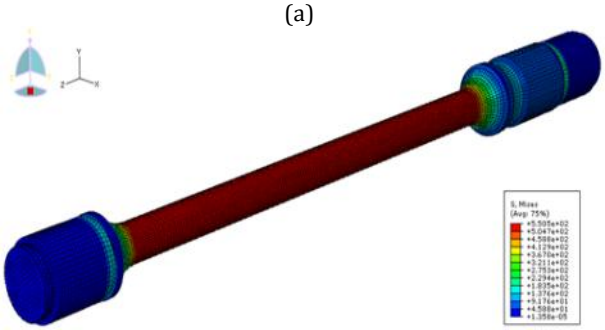

(b)

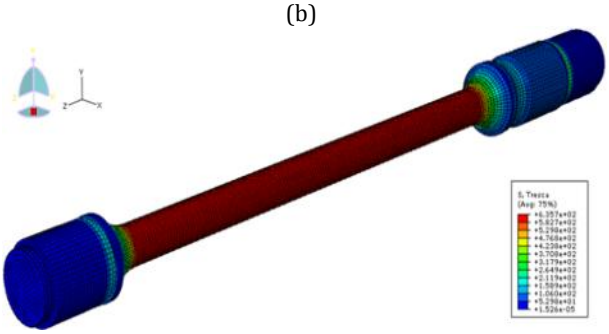

Figure 11: FE results including (a) the Von-mises stress and (b) the Tresca stress

Table 3: FE results of the coupling system under various loading conditions

State	Torque (Nm)	Misalignment (mm)	Tresca stress (MPa)	Von-mises stress (MPa)
1	400	0.0	635.7	550.5
2	400	0.2	635.8	550.6
3	500	0.0	794.7	688.2
4	400	20.0	729.6	661.3

To simulate the reality of loadings, a fatigue analysis was carried out on the model. The cyclic loading type of the coupling system is in the high cycle fatigue (HCF) regime. The strategy of engine stops in the dynamometer is a reverse revolution, when the engine is working. Therefore, the loading history of the coupling can be drawn as Figure 12. When the engine works, there may be several fluctuations in the torque.

In addition, there is a negative value for the torque, since for stopping the engine (the shut-down state), the dynamometer applies a reverse torque (unlike the engine rotation direction) on the engine. If the start-up duration is not considered, between the time of engine working and the shut down time, we can say that loading conditions will be assumed to be a fully reversed loading condition with zero mean stress.

The endurance fatigue limit of the alloy was considered as 529 MPa at 10^7 cycles [5]. This limit in torsional conditions becomes 305.4 MPa, but the coefficient of the fatigue strength (the power of the stress-life relation) was not changed [9]. Therefore, the fatigue lifetime of the coupling could not be infinity based on the Tresca criterion and the coupling system had a limited lifetime.

To find the endurance fatigue limit in real conditions (S_e), Equation (2) can be used as following [9],

$$S_e = k_a k_b k_c k_d k_e k_f S'_e \quad (2)$$

In which, S'_e is the endurance fatigue limit obtained from rotary bending HCF tests. This value should be changed to torsional loadings by a factor, which was 0.577 [9]. Other parameters are correction factors for the surface, the size, the loading type, the temperature, the reliability and the stress concentration, respectively.

Considering 862 MPa for the ultimate strength of the alloy [5], the surface factor could be regarded as 0.75 for the machined shaft [10]. As the shaft diameter was 19.7 mm, the size factor could be calculated as 0.90 and the loading factor was 0.59 due to torsional loadings [10]. Diameters (d and D) of the shaft are changed from 37.5 mm to 19.7 mm by a fillet radius (r) of 25 mm. Thus, the ratios of r/d and D/d are calculated as 1.27 and 1.90, respectively. Consequently, the correction factor for the stress concentration effect becomes 0.91 [9]. In this fatigue analysis, the temperature factor and the reliability factor are considered as 1 for the coupling system. By applying values of correction factors to Equation (2), the endurance fatigue limit could be calculated as 192.5 MPa. As a result, the safety factor becomes 0.35 and 0.30 based on Von-mises and Tresca criteria, respectively.

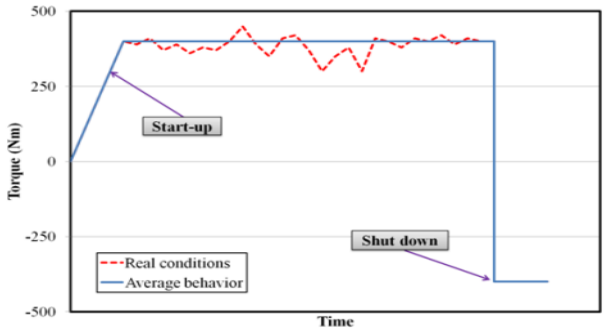

Figure 12: The schematic loading history in the coupling system

To find the fatigue lifetime (N_f), Equations (3) and (4) can be used as following [10],

$$S_f = a\left(N_f\right)^b \quad (3)$$

$$a = \frac{\left(fS_u\right)^2}{S_e}, b = -\frac{1}{3}\log\left(\frac{fS_u}{S_e}\right) \quad (4)$$

In which, S_u is the ultimate strength of the alloy. The value of f could be calculated as 0.815 by considering 862 MPa for the ultimate strength of the alloy [4]. Consequently, a and b coefficients will be equal to 2563.3 MPa and -0.187, respectively. When a 400 Nm torque was applied on the coupling model, the fatigue lifetime, based on the Von-mises estimation will be 3675 cycles, whereas by means of the Tresca calculation would not exceed 1705 cycles. Other fatigue lifetimes under various loading conditions are shown in Table 4. These results demonstrate that by the 25% increase in the torque value, the fatigue lifetime becomes equal to one third of the initial state and it will drastically reduce by 50%, while the misalignment increases a hundredfold.

Therefore, in the part of mechanical investigations, we could say that:

- Checking the vibration behavior (including the natural frequency) demonstrated that the critical speed was 438 rpm, below the idle speed of the engine, which was about 800 rpm. If the duration time of passing this speed during engine starting is not so low, the resonance will be occurred.
- Checking the vibration spectrum (including the transient behavior) of the component showed that the vibration velocity was lower than the value, mentioned in the specification.
- Checking the stress of the component illustrated that the safety factor was higher than 1, which was satisfactory.
- Checking the fatigue lifetime of the component under various critical loading showed that the misalignment had lower effect on the fatigue lifetime, in comparison to the enhancement of the torque.

Table 4: The fatigue lifetime of the coupling system under various loading conditions

State	Amount of Increase (%) in stress		Fatigue lifetime (cycle) based on	
	Tresca stress	Mises stress	Tresca stress	Mises stress
1	Initial state	Initial state	1705	3675
2	0.2	0.2	1703	3671
3	25	25	518	1116
4	15	20	817	1381

3.3) Fishbone Analysis and Failure Causes

Based on mentioned root causes of the shaft failure in the fishbone diagram and according to both material and mechanical investigations, for each branch of the fishbone, we could say that:

- Material defect branch: The failure was no due to the material.
- Imbalance and misalignment branches: Their effect was less than the effect of the torque enhancement on the fatigue lifetime. However, they could be one cause of the failure.
- Coupling selection branch: It was not checked in this research and it was supposed to be correctly selected.
- Vibration branch: No extra vibration was observed. However, the critical speed was less than the idle speed of the engine and this passing the critical speed was the cause of the failure. Since the time duration of passing this speed was not so low, when engines have been started. This would be caused to the resonance phenomenon.
- Fatigue branch: Since the working hour of four failed shafts was not the same, the fatigue lifetime of the component was not the main cause of the failure. However, it was terminate, when the torque and the misalignment increased. Besides, it was shown that the torque enhancement beside the misalignment had a significant effect on the lifetime reduction.

Consequently, we predicted two root causes for the failure of the coupling shaft including the critical speed (especially the high passing time of the engine start) and the misalignment. Therefore, vibration monitoring would be a proper suggestion to prevent such there failures in the coupling system of dynamometers.

4) Conclusions

In this research, a failure analysis of an engine test bed, includes a failed coupling system, has been carried out. For this purpose, material and mechanical investigations were performed based on the fishbone diagram. Obtained results showed that no material defect was observed. SEM images demonstrated cleavage marks under fatigue loadings. The critical speed of the coupling system was calculated as 438 rpm, which has been placed below the idle speed of internal combustion engines. To prevent failures, the engine should run quickly in order to avoid possible resonance. Unfortunately, this caution was not done properly and thus, the critical speed was a cause of the failure. Another failure cause was the fatigue lifetime reduction according to the misalignment. In other words, misalignments higher than allowable values could severely decrease the lifetime. Based on this important point, we suggest an accurate alignment device to monitor the system during engine testing.

Acknowledgment

Authors should like to extend their thanks to Irankhodro Powertrain Company (IPCO) includes the vehicle/engine laboratory for their financial supports in experiments, and in particular, Mr. Sharghi, Mr. Tahi, Mr. Zakeri, Mr. Noori, Mr. Ghassami and Mr. Salimi.

References

[1] A.J. Martyr, M.A. Plint, Engine testing - theory and practice, Elsevier Ltd., UK, 2007

[2] V. Venkateswarlu, D. Tripathy, K. Rajagopal, K.T. Tharian, P.V. Venitakrishnan, Failure analysis and optimization of thermo-mechanical process parameters of titanium alloy (Ti-6Al-4V) fasteners for aerospace applications, Case Studies in Engineering Failure Analysis, Vol. 1, pp. 49-60, 2013

[3] Standard specification for titanium and titanium alloy bars, Standard Number ASTM B348-06a, 2006

[4] Standard test method for Brinell hardness test of metallic materials, Standard Number ASTM-E10-06, 2006

[5] Properties and selection: Nonferrous alloys and special-purpose materials, Vol. 2, ASM Metals Handbook, 1990

[6] Metallography and micro-structures, Vol. 9, ASM Metals Handbook, 1990

[7] Failure analysis and prevention, Vol. 11, ASM Metals Handbook, 1990

[8] Assembly and operating manual - compact coupling shaft series 900, AVL Company, 2005

[9] D.F. Socie, G.B. Marquis, Multiaxial fatigue, SAE International, USA, 2000

[10] R. Budynas, K. Nisbett, Shigley's mechanical engineering design, McGraw-Hill Primis, 2006

فصلنامهٔ علمی- پژوهشی تحقیقات موتور

تارنمای فصلنامه: www.engineresearch.ir

گزارش فنی

تحلیل خرابی محور اصلی لگام ترمز متصل به موتور

محمد آزادی[۱*]، رضوان روحانی[۲]، مهدی روزبان[۳]، امیر مافی[۴]

[۱] شرکت تحقیق، طراحی و تولید موتور ایران‌خودرو (ایپکو)، تهران، ایران، m_azadi@ip-co.com
[۲] شرکت تحقیق، طراحی و تولید موتور ایران‌خودرو (ایپکو)، تهران، ایران، r_rohani@ip-co.com
[۳] شرکت تحقیق، طراحی و تولید موتور ایران‌خودرو (ایپکو)، تهران، ایران، m_roozban@ip-co.com
[۴] شرکت تحقیق، طراحی و تولید موتور ایران‌خودرو (ایپکو)، تهران، ایران، a_mafi@ip-co.com
[*] نویسندهٔ مسئول، شمارهٔ تماس: ۰۹۱۰۲۱۰۷۲۸۰

چکیده

در این مقاله، تحلیل خرابی محور لگام ترمز با چهار دفعه تکرار شکست، ارائه می‌شود. برای تحلیل خرابی، بررسی مواد با استفاده از عکس‌های میکروسکوپ الکترونی روبشی انجام شد. به علاوه، ریزساختار محور آسیب دیده، عکس‌برداری شد؛ سختی آن نیز اندازه‌گیری گردید و با خواص ماده مرجع، مقایسه شد. همچنین، با استفاده از شبیه‌سازی ناهم‌محوری در یک الگوی اجزاء محدود، عمر خستگی آن بر اساس محدودهٔ خستگی پربسامد و حد دوام خستگی قطعه، محاسبه گردید. احتمال تأثیر ارتعاش پیچشی و پدیدهٔ تشدید نیز، مطالعه شد. در انتها، با مقدار ارتعاشات و محدودهٔ مجاز دامنهٔ ارتعاشی، مقایسه گردید. عکس‌های ذره‌بین برقی روبشی (SEM)، اثرات رخ‌برگی (cleavage) را تحت بارهای خستگی نشان دادند. این اثرات، گویای شکست شکننده ماده‌اند. ریزساختار به همراه سختی ماده، مشکلی نداشت. براساس نتایج عددی، در عمر خستگی محور، به دلیل افزایش ناهم‌محوری، به عنوان یک عامل خرابی، مشکلی وجود داشت. عامل دیگر خرابی می‌توانست پدیدهٔ تشدید و سرعت بحرانی محور باشد که کمتر از دور آرام موتور، محاسبه شد.

اطلاعات مقاله

تاریخچهٔ مقاله:
دریافت: ۰۲ آبان ۱۳۹۲
پذیرش: ۰۳ دی ۱۳۹۲

کلیدواژه‌ها:
تحلیل خرابی
محور لگام ترمز
عمر خستگی
ناهم‌محوری
تشدید